ACCOUNTS
of chemical research

Nanostructured Catalysts for Organic Transformations

LENG LENG CHNG, NANDANAN ERATHODIYIL, AND JACKIE Y. YING*

Institute of Bioengineering and Nanotechnology, 31 Biopolis Way, The Nanos, Singapore 138669

RECEIVED ON JULY 5, 2012

CONSPECTUS

The development of green, sustainable and economical chemical processes is one of the major challenges in chemistry. Besides the traditional need for efficient and selective catalytic reactions that will transform raw materials into valuable chemicals, pharmaceuticals and fuels, green chemistry also strives for waste reduction, atomic efficiency and high rates of catalyst recovery.

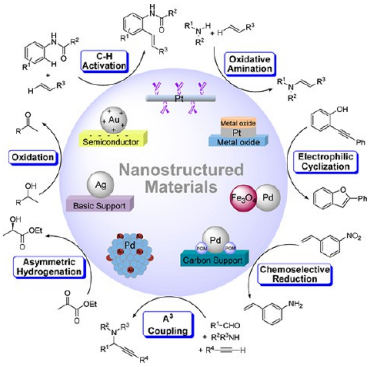

Nanostructured materials are attractive candidates as heterogeneous catalysts for various organic transformations, especially because they meet the goals of green chemistry. Researchers have made significant advances in the synthesis of well-defined nanostructured materials in recent years. Among these are novel approaches that have permitted the rational design and synthesis of highly active and selective nanostructured catalysts by controlling the structure and composition of the active nanoparticles (NPs) and by manipulating the interaction between the catalytically active NP species and their support. The ease of isolation and separation of the heterogeneous catalysts from the desired organic product and the recovery and reuse of these NPs further enhance their attractiveness as green and sustainable catalysts.

This Account reviews recent advances in the use of nanostructured materials for catalytic organic transformations. We present a broad overview of nanostructured catalysts used in different types of organic transformations including chemoselective oxidations and reductions, asymmetric hydrogenations, coupling reactions, C–H activations, oxidative aminations, domino and tandem reactions, and more. We focus on recent research efforts towards the development of the following nanostructured materials: (i) nanostructured catalysts with controlled morphologies, (ii) magnetic nanocomposites, (iii) semiconductor–metal nanocomposites, and (iv) hybrid nanostructured catalysts. Selected examples showcase principles of nanoparticle design such as the enhancement of reactivity, selectivity and/or recyclability of the nanostructured catalysts via control of the structure, composition of the catalytically active NPs, and/or nature of the support. These principles will aid researchers in the rational design and engineering of new types of multifunctional nanocatalysts for the achievement of green and sustainable chemical processes.

Although the past decade has brought many advances, there are still challenges in the area of nanocatalysis that need to be addressed. These include loss of catalytic activity during operation due to sintering, leaching of soluble species from the nanocatalysts under harsh reaction conditions, loss of control over well-defined morphologies during the scale-up synthesis of the nanocomposites, and limited examples of enantioselective nanocatalytic systems. The future of nanocatalyst research lies in the judicious design and development of nanocomposite catalysts that are stable and resistant to sintering and leaching, and yet are highly active and enantioselective for the desired catalytic organic transformations, even after multiple runs. The successful generation of such multifunctional nanocatalysts especially in tandem, domino, or cascade reactions would provide a powerful tool for the establishment of green and sustainable technologies.

Introduction

The catalytic efficiency, selectivity, and recyclability of nanocatalysts depend on the size, shape, composition, and assembly of the nanoparticles (NPs), as well as their interaction with the support. These fascinating phenomena enhance the appeal of well-defined nanostructured materials as green and sustainable heterogeneous catalysts in a wide variety of organic transformations. Nanocatalysts may be designed as nanocrystals and clusters of metals, metal oxides, and nonoxides of various sizes and shapes.

Published on the Web 01/25/2013 www.pubs.acs.org/accounts
10.1021/ar300197s

They may involve no support material or be supported on carbonaceous materials, polymers, metal oxides, or porous materials (e.g., siliceous mesocellular foam (MCF)). The latest direction for green and sustainable reactions using nanocatalysts is exciting scientifically, and much has been achieved in the past decade in the synthesis as well as the catalytic applications of nanostructured materials.

In this Account, we aim to present a broad overview of nanostructured catalysts used in different types of organic transformations. Selected examples would be used to highlight the concepts behind the enhancement of the reactivity, selectivity, and/or recyclability of the nanostructured catalysts through the control of the structure, composition of the catalytically active NPs, and/or nature of the support. Our focus would be on recent research efforts (2006 to present; readers interested in earlier work are directed to selected reviews[1]) toward the development of the following nanostructured materials used in organic catalysis (excluding electrocatalysis and photocatalysis).

(i) *Nanostructured catalysts with controlled morphologies*. Catalysis for this class of nanomaterials is controlled by the crystallite size and morphology (Scheme 1A). The catalytic performance can be enhanced by the presence of a particular crystal facet or the creation of uncoordinated surface atoms in the nanocrystal. Modification of a crystal facet with a chiral ligand would in turn yield active heterogenized catalyst for enantioselective reactions.

(ii) *Magnetic nanocomposites*. Magnetic nanocomposites either can catalyze the organic transformation on their own or can serve as an effective support for the immobilization of active catalysts (Scheme 1B). The efficient recovery of the catalyst by magnetic separation would further enhance the recovery and reuse of these nanocomposites and their attractiveness as green catalysts. Modification of the surface of active NPs with chiral ligands could impart chirality.

(iii) *Semiconductor-metal nanocomposites*. For these nanocomposite materials, the semiconductor can either withdraw electrons from or donate electrons to the metal NPs (Scheme 1C). The resulting positively or negatively charged metal NPs can then catalyze different organic transformations. Semiconductor metal oxide based nanomaterials can also serve as a support, providing either basic or acidic sites in close proximity to the active metal NPs. The synergism between the active metal NPs and the basic or acidic support would then catalyze organic reactions.

(iv) *Hybrid nanostructured catalysts*. A variety of hybrid nanostructured materials has been developed (Scheme 1D). In some cases, the metal NPs can become active by being in close contact with an oxidant (e.g., polyoxometalate), thus catalyzing oxidative coupling reactions. In other cases, the hybrid nanostructured material may consist of isolated metal atom geometries, yielding individual atoms that are catalytically active. Bimetallic NPs displaying synergistic effects and multifunctional nanostructured catalysts for tandem reactions have also been reported.

Nanostructured Catalysts with Controlled Morphologies

The control over crystal size and morphology to tailor the catalytic properties has gained increased attention in recent years.[1e,2] Synthesis and reactivity of palladium (Pd) NPs that are either colloidally stabilized or supported on various materials have been extensively studied.[3]

The correlation of activity and selectivity of structure-sensitive reactions with the shape and size of the nanocrystalline catalyst was exploited for rational catalyst design by Crespo-Quesada et al.[4] In this work, uniform Pd nanocrystals with cubic (CUB), octahedral (OCT), and cuboctahedral (COT) shapes were synthesized and then used for the hydrogenation of 2-methyl-3-butyne-2-ol (eq 1). Two types of active sites were involved in the catalysis: semihydrogenation preferentially occurred at the planes, whereas overhydrogenation took place mainly at the edges. Surface statistics for nanocrystals with different sizes and shapes showed that the optimal catalyst in terms of yield of the target product was cubes with ~3−5 nm in edge length.

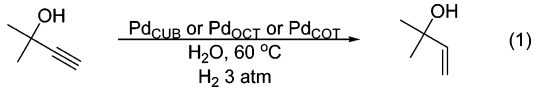

(1)

Platinum (Pt) NPs with an average size distribution of 0.8−1 nm but different shapes were studied and found to display distinct reactivity for the oxidation of propan-2-ol (eq 2).[5] A correlation between the number of uncoordinated atoms at the NP surface and the onset temperature for propan-2-ol oxidation was observed, demonstrating that catalytic properties could be controlled through shape-selective synthesis. In another example, Hong et al. developed an efficient synthesis of Pt@Fe_2O_3 nanowires, and demonstrated the utility of the iron oxide coated platinum nanowires in the selective oxidation of olefins and alcohols (eqs 3 and 4).[6]

SCHEME 1. Catalysis with Nanostructured Materials

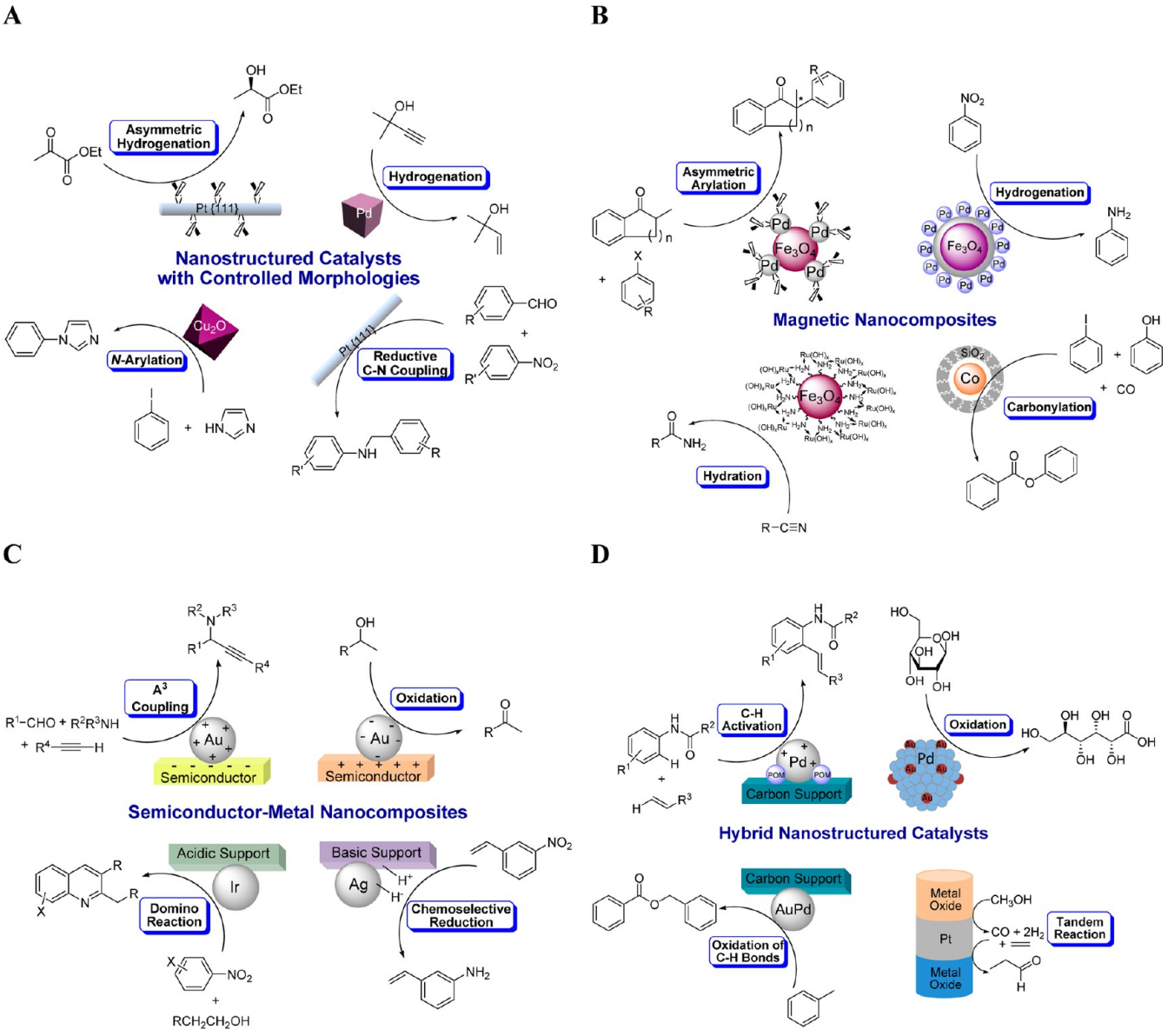

$Pt@Fe_2O_3$ nanowires exhibited far higher activity than the Fe_2O_3 and $Pt@Fe_2O_3$ NPs due to the interface between Fe_2O_3 and Pt nanowires, which served as the active center for activating oxygen (O_2).

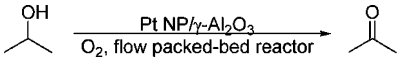

(2)

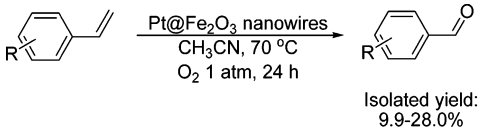

(3)

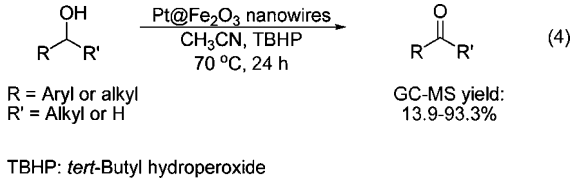

(4)

TBHP: *tert*-Butyl hydroperoxide

Pt, ruthenium (Ru), rhodium (Rh) and iridium (Ir) NPs are widely used in hydrogenation reactions.[7] The structure sensitivity of enantioselective hydrogenations on chirally modified metals was investigated using Pt NPs of different shapes such as cubic, cuboctahedral, and octahedral (eq 5).[8] This study revealed for the first time that enantioselective hydrogenation on chirally modified Pt NPs was

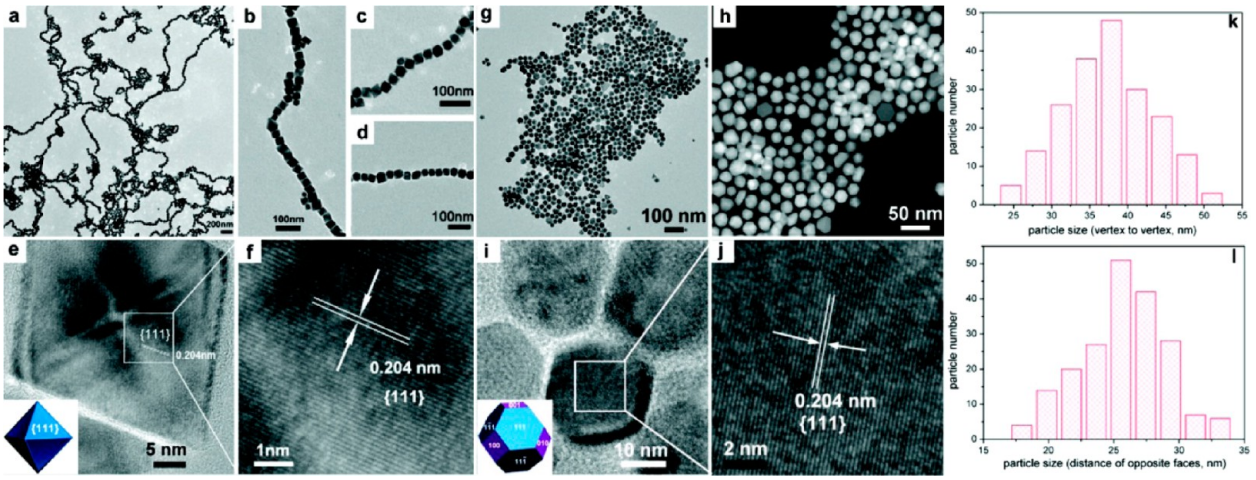

FIGURE 1. (a) Transmission electron microscopy (TEM) image of Ni octahedrons. (b–d) Magnified TEM images of Ni 1D structures with different orientation. (e) High-resolution TEM (HRTEM) image of Ni octahedron; the inset is the scheme of the structure of octahedron. (f) Magnified images of the lattice fringe of the Ni octahedron. (g) TEM and (h) high-angle annular dark-field scanning transmission electron microscopy (HAADF-STEM) images of Ni truncated octahedrons. (j) Magnified images of the lattice fringe of the Ni truncated octahedron in (i). Size distributions of (k) octahedral Ni nanoparticles and (l) truncated octahedral Ni nanoparticles. Reprinted with permission from ref 9. Copyright 2012 American Chemical Society.

shape-selective: both the reaction rate and the enantioselectivity increased with an increase in the Pt{111}/Pt{100} ratio. Recently, a general method to synthesize water-soluble octahedral, truncated octahedral, and cubic Pt, Pt_xNi_{1-x}, and nickel (Ni) nanocrystals with uniformly controlled shapes and compositions was reported (Figure 1).[9] Structure–activity dependence studies revealed that the shapes, compositions, and capping agents strongly influenced the catalytic performances in hydrogenation reactions (eq 6). The higher catalytic performance for $PtNi_2$ octahedron was ascribed to a higher percentage of exposed {111} facets.

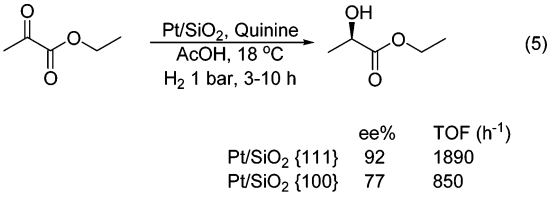

(5)

	ee%	TOF (h^{-1})
Pt/SiO_2 {111}	92	1890
Pt/SiO_2 {100}	77	850

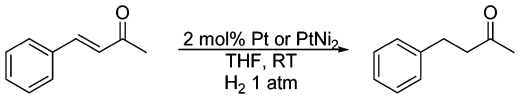

(6)

	TOF (h^{-1})
Pt octahedron	23
$PtNi_2$ octahedron	139
$PtNi_2$ truncated octahedron	114
$PtNi_2$ cube	95

THF: Tetrahydrofuran

We have developed ultrathin Pt nanowires with a diameter of 1 nm and a length of 100 nm.[10] The surface of the Pt nanowires was modified with cinchona alkaloid and used for hydrogenation of α-ketoesters at room temperature and under low pressure in water (eq 7). The catalysts showed excellent yields and moderate-to-excellent enantioselectivities, and provided ease of handling under moisture and air. They were easily recycled, without any change in activity, and showed only a minor change in selectivity (1–5% enantiomeric excess (ee)) over 11 runs (Figure 2). These Pt nanowires were also used by Hu et al. for the efficient C–N coupling of carbonyls with aromatic nitro compounds under low hydrogen (H_2) pressure to *N*-alkylamines (eq 8).[11] They exhibited a much higher catalytic activity than Pt NPs or nanorods due to the predominance of the Pt{111} surfaces.

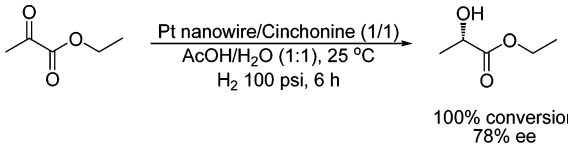

(7)

100% conversion
78% ee

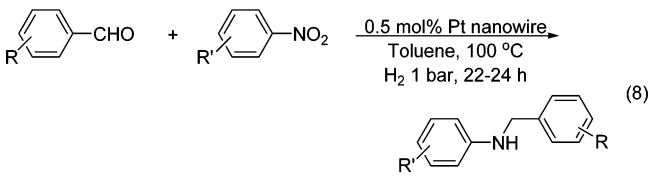

(8)

Isolated yield:
67-95%

Cuprous oxide (Cu_2O) nanocrystals of cubic, octahedron-like, sphere-like, plate-like, and cuboctahedron-like morphologies have been synthesized. They were examined in

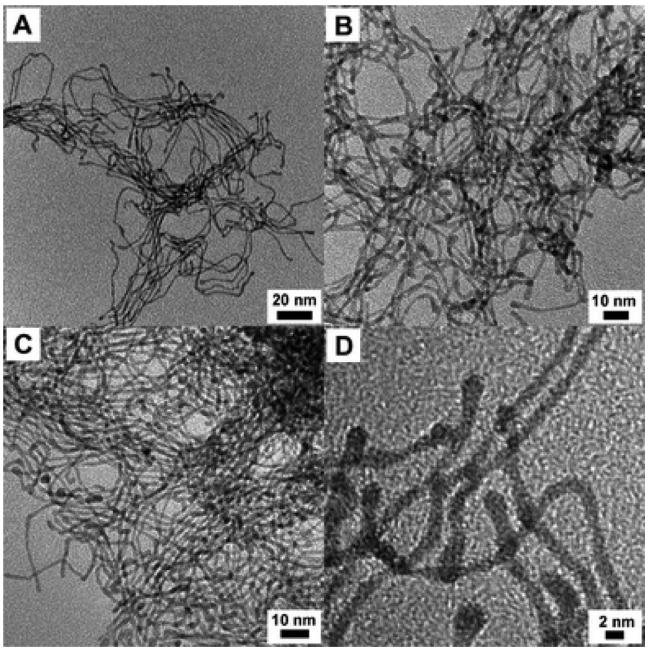

FIGURE 2. (A–C) TEM and (D) high-resolution TEM images of Pt nanowires (A) before use, (B) after 2 runs, and (C, D) after 10 runs. Reprinted with permission from ref 10. Copyright 2011 Royal Chemical Society.

N-arylation reactions (eq 9) and clearly demonstrated the shape and morphology dependency of catalytic sites.[12] {111} planes of Cu_2O showed a higher catalytic activity than {100} planes and nanospheres due to surface atomic densities, surface energies, and electronic surface properties. Pd concave nanocubes with high-index faces were fabricated by Jin et al. and employed in the Suzuki coupling reaction (eq 10).[13] Compared to the Pd nanocubes enclosed by {100} facets, the Pd concave nanocubes enclosed by high-index {730} facets displayed a substantially higher catalytic activity.

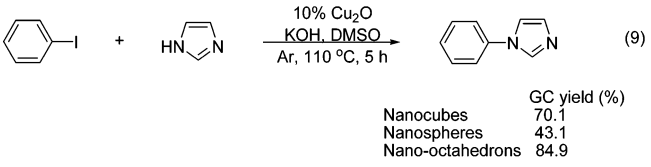

	GC yield (%)
Nanocubes	70.1
Nanospheres	43.1
Nano-octahedrons	84.9

DMSO: Dimethylsulfoxide

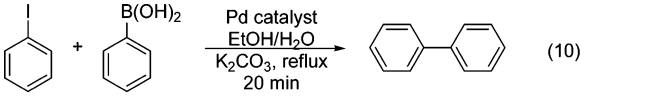

	GCMS yield (%)
Pd nanocubes	38
Pd concave nanocubes	99

Magnetic Nanocomposites

Magnetic NPs have been extensively explored as alternative catalyst supports due to their high surface area (resulting in high catalyst loading capacity), high dispersion, excellent stability, and ease of catalyst recycling.[14] The catalysts are usually immobilized on the surface of the magnetic NPs, allowing for easy access to the active sites. Recovery of the catalyst from liquid phase reactions by magnetic separation is more conveniently achieved than conventional methods, such as filtration or centrifugation. Iron oxide NPs such as magnetite (Fe_3O_4) and maghemite (γ-Fe_2O_3) are commonly used as catalyst supports, and the catalysts are generally loaded onto the magnetic support either by further surface modification of the magnetic NPs (MNPs) or by coprecipitation with MNPs during synthesis whereby functional ligands are used as stabilizers.[15]

We have demonstrated the use of SiO_2/Fe_2O_3 nanocomposites as a magnetic catalyst support whereby Pd nanoclusters were deposited in high dispersion and stability.[16] The catalyst was used for the hydrogenation of nitrobenzene with excellent reactivity and reusability (eq 11, Figure 3). The excellent reactivity and recyclability of the Pd/H_2N–SiO_2/Fe_2O_3 (99% yield over 6 runs) was due to the amine ligands on SiO_2/Fe_2O_3, which suppressed the agglomeration of Pd nanoclusters during the hydrogenation reaction.

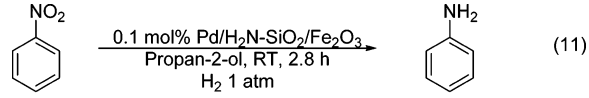

100% conversion

γ-Fe_2O_3 NPs could also be grown inside MCFs, which showed a high surface area and a large pore size, facilitating the loading of, reaction with and recycling of enzyme catalysts, Pd nanoclusters (eq 12) and Ru-based catalysts.[17]

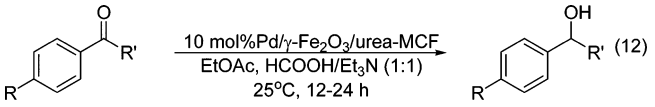

Isolated yield: 84-99%

Various noble metal nanocatalysts, such as Pt, gold (Au) and Pd, were directly grown on the surface of Fe_3O_4/SiO_2 or polymer nanotube magnetic hybrids with high dispersion and high loading capacity. High catalytic activity was observed in the reduction of nitrophenol (eq 13), alcohol oxidation (eq 14), and Heck coupling reactions (eq 15) with high activity and recyclability.[18]

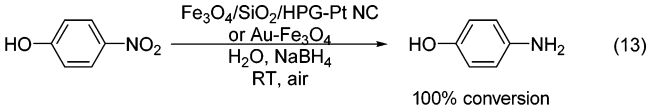

100% conversion

HPG: Hyperbranched polyglycerol

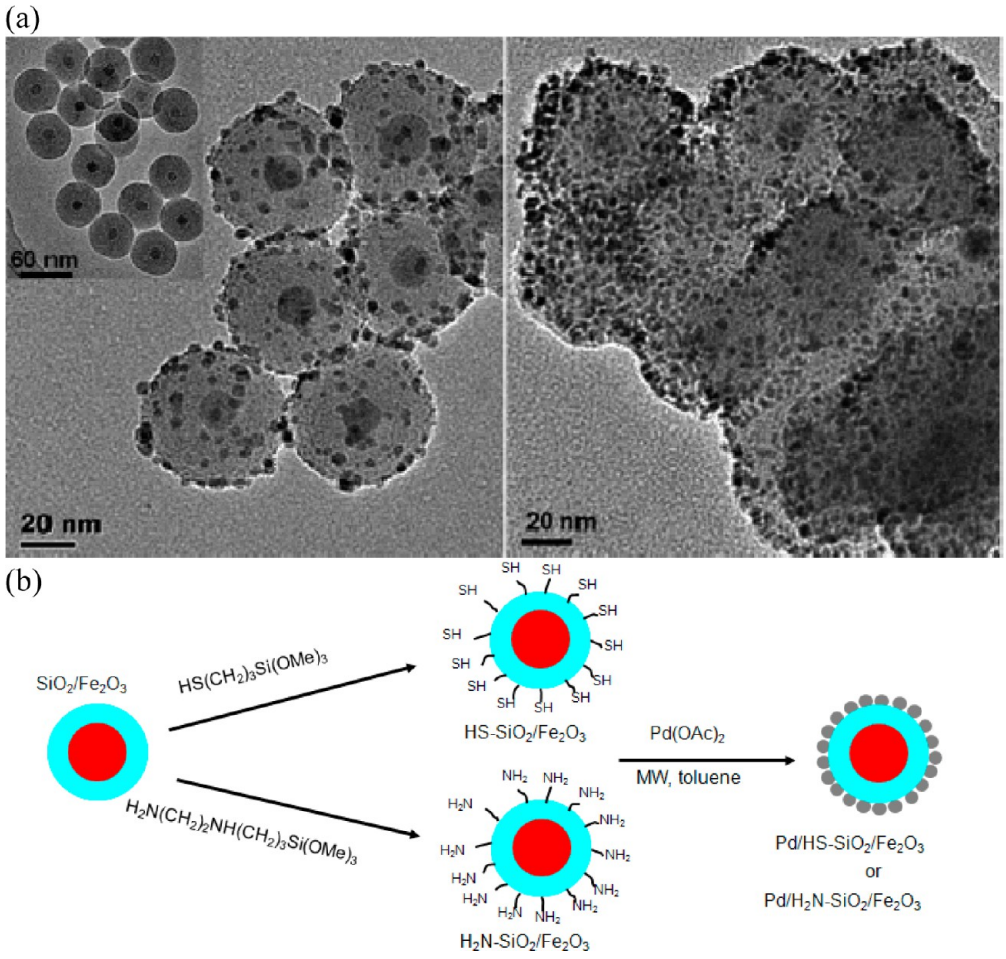

FIGURE 3. (a) TEM micrographs of as-prepared SiO_2/Fe_2O_3 (left inset), Pd/HS-SiO_2/Fe_2O_3 (left), and Pd/H_2N-SiO_2/Fe_2O_3 (right). (b) Synthesis of Pd/SiO_2/Fe_2O_3 nanocomposites. Reprinted with permission from ref 16. Copyright 2006 American Chemical Society.

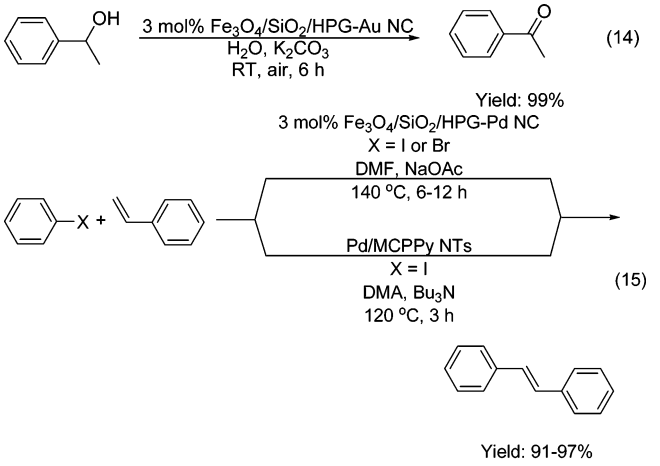

MCPPy NTs: Magneric carboxylated polypyrrole nanotubes

An environmentally friendly magnetically recoverable iron oxide nanocatalyst was used as efficient catalyst for the synthesis of 2-phenylquinazolines under solvent-free conditions by Anand et al. (eq 16).[19] A gram-scale synthesis of magnetically separable and recyclable Co@SiO_2 yolk-shell nanocatalyst was reported by Park et al., and this catalyst was efficiently used for the phenoxycarbonylation of iodobenzene (eq 17).[20] This nanocatalyst owed its high activity to surface cleanness and individual protection of the cobalt (Co) cores against sintering. A nanoferrite-supported ruthenium hydroxide catalyst showed excellent reactivity in the hydration of nitriles (eq 18), which proceeded in aqueous medium (Figure 4).[21] The noncovalent anchoring of the ruthenium hydroxide to the amine-binding sites on the surface of the nanoferrite minimized deterioration and metal leaching, and permitted efficient catalyst recycling. Novel bimetallic Cu@Fe NPs acted as a recoverable heterogeneous catalyst for the azide–alkyne click reaction in water in excellent yield (eq 19),[22] and copper ferrite NPs were used for cross-coupling of aryl halides with diphenyl selenides (eq 20).[23]

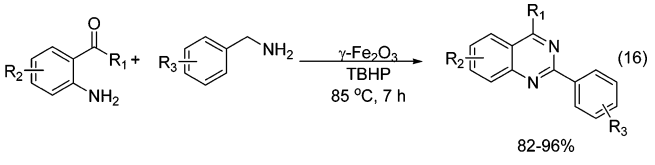

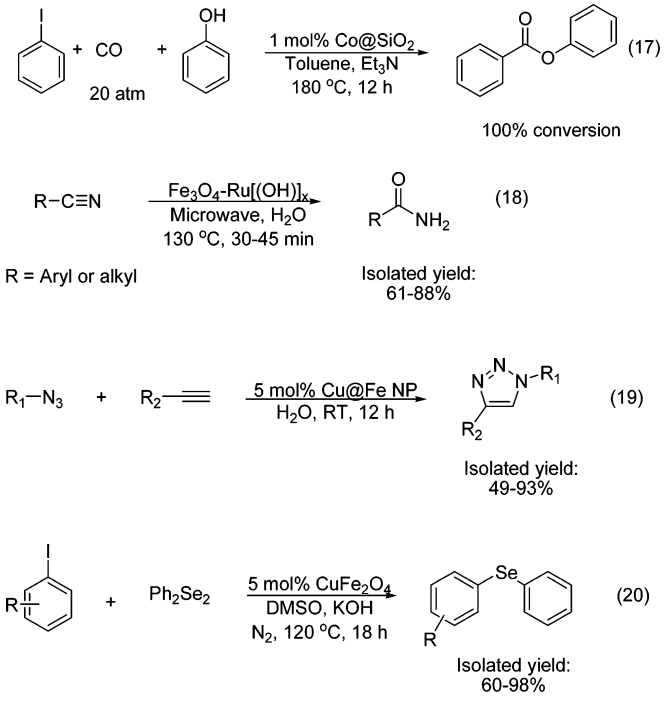

Ranganath et al. reported the formation of Pd NPs on Fe_3O_4 and subsequent chiral surface modification using enantiomerically pure *N*-heterocyclic carbenes (NHCs).[24] The chiral NHCs bearing secondary hydroxyl groups not only acted as chiral modifiers for the Pd NPs, but also stabilized the Pd NPs against leaching. This readily accessible catalyst was successfully applied in asymmetric heterogeneous α-arylation of ketones, yielding up to 85% ee with excellent catalyst recyclability (eq 21, Figure 5).

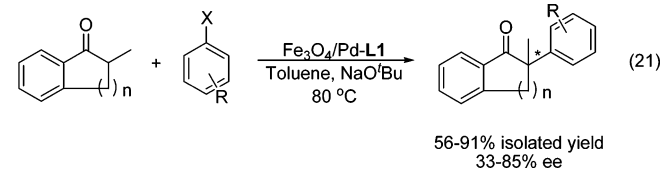

Hu et al. designed and synthesized MNP-supported chiral catalysts containing 4,4′-bisphosphonic-acid-substituted BINAP-Ru-DPEN (BINAP = [1-(2-diphenylphosphanylnaphthalen-1-yl)naphthalen-2-yl]-diphenylphosphane, DPEN = (*R*,*R*)-1,2-diphenylethylenediamine) moieties, and employed them in the asymmetric hydrogenation of ketones with excellent conversions and enantioselectivities (eq 22).[25] FePd modified by chiral BINAP was used for an asymmetric coupling reaction (eq 23).[26] The BINAP ligand served a dual function of imparting chirality to the NPs and acting as a stabilizer to prevent sintering and agglomeration under catalytic conditions.

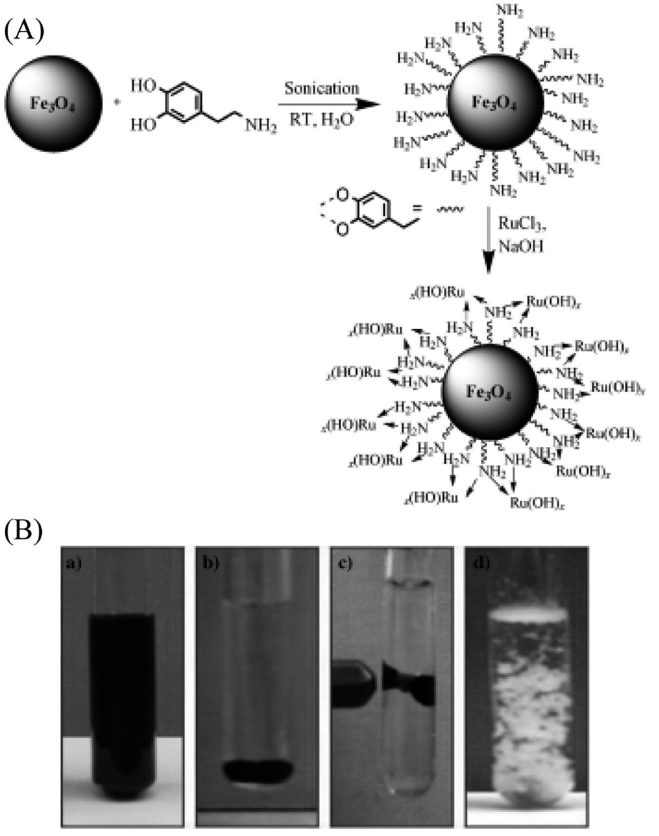

FIGURE 4. (A) Synthesis of nanoferrite−[Ru(OH)]$_x$. (B) Hydration of benzonitrile to benzamide using nanoferrite−[Ru(OH)]$_x$ catalyst. Photographs of the glass tube: (a) during reaction under stirring, (b) after reaction completion without stirring, (c) catalyst removal by external magnet, and (d) appearance of product crystals after cooling the aqueous solution. Reprinted with permission from ref 21. Copyright 2009 Wiley-VCH Verlag GmbH & Co. KGaA.

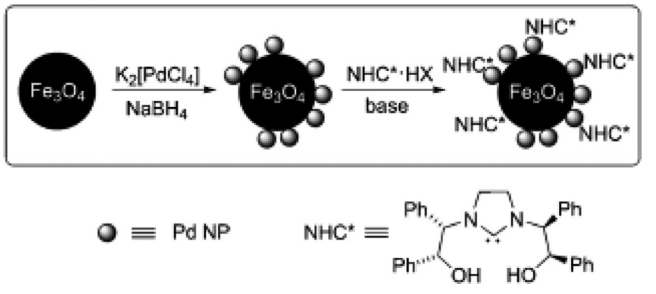

FIGURE 5. Preparation of Fe_3O_4/Pd NPs modified by chiral NHC; for clarity, the sizes are not represented in proportion. Reprinted with permission from ref 24. Copyright 2010 Wiley-VCH Verlag GmbH & Co. KGaA.

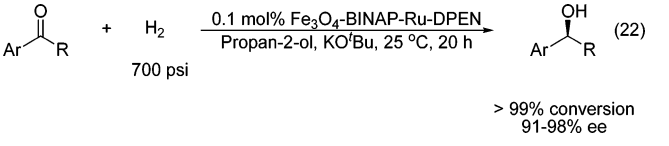

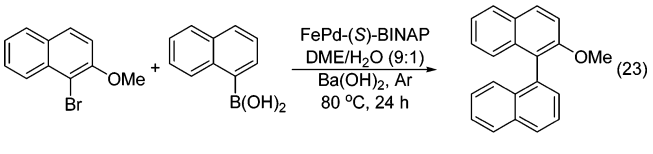

DME: 1,2-Dimethoxyethane

Semiconductor-Metal Nanocomposites

Supported Au/CeO_2 and Au/ZrO_2 catalysts have been synthesized for a highly efficient three-component coupling reaction of aldehydes, amines, and alkynes/N-protected ethynylanilines (A^3 coupling) in water to produce substituted propargylamines and indoles in good-to-excellent yields (eqs 24 and 25).[27] The high activities of the heterogeneous catalysts have been attributed to the stabilization of the active cationic Au(III) species on cerium oxide (CeO_2) or zirconium oxide (ZrO_2).

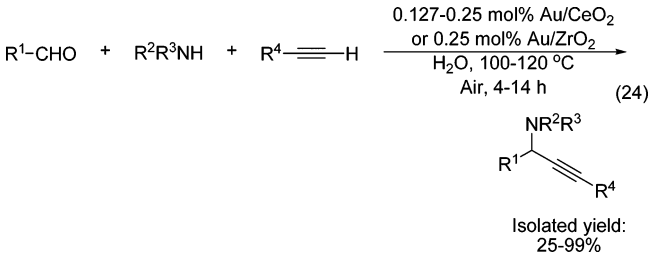

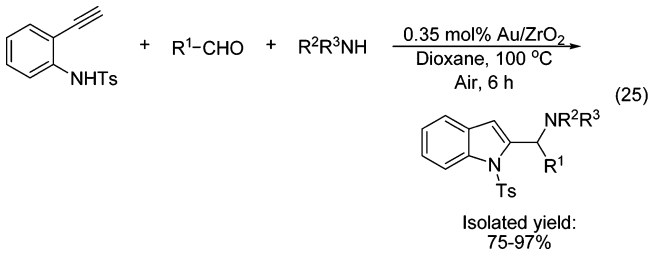

Wang et al. have used a supported Au/MoO_x heterogeneous catalyst for the aerobic oxidation of alcohols to aldehydes in high yields (eq 26).[28] In their study, the authors confirmed that electron transfer from the partially reduced MoO_x support to the Au NPs would result in negatively charged Au cores, yielding highly active catalysts for the selective aerobic oxidation of alcohols. In a related earlier study, Au clusters smaller than 1.5 nm stabilized by poly(*N*-vinyl-2-pyrrolidinone) (PVP) were used as active catalysts for the aerobic oxidation of alcohol to aldehyde (eq 27).[29] The catalytically active Au clusters were negatively charged by electron donation from PVP, and the catalytic activity of the Au clusters was enhanced with increasing electron density on the Au core.

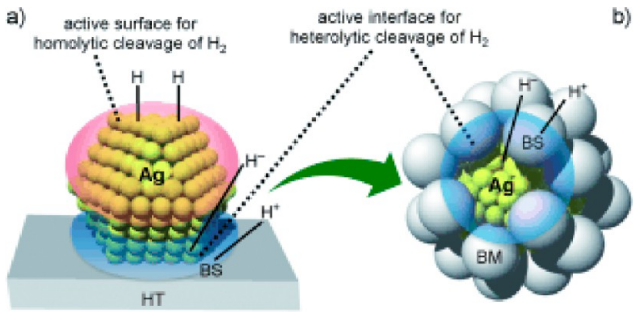

FIGURE 6. Catalyst design of core–shell nanocomposite for chemoselective reductions with H_2. (a) Representation of Ag/HT reacting with H_2; both polar and nonpolar hydrogen species are formed. (b) Representation of AgNPs@BM; AgNPs are covered with a basic material (BM), which reacts with H_2 at a basic site (BS) to result in the exclusive formation of polar hydrogen species. Reprinted with permission from ref 31. Copyright 2012 Wiley-VCH Verlag GmbH & Co. KGaA.

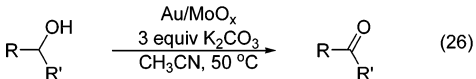

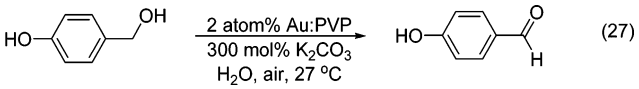

Mitsudome et al. have exploited Au and silver (Ag) NPs supported on hydrotalcite (HT) as highly active catalysts for the deoxygenation of epoxides to alkenes using alcohol as a reductant (eq 28).[30] Excellent selectivities (of >99%) and turnover numbers (up to 20 000) were achieved. Based on their experimental results, the authors proposed that the basic support hydrotalcite promoted the deoxygenation of epoxides by providing the basic sites required for the oxidation of alcohols to produce metal hydride ($[H-Au]^-$ or $[H-Ag]^-$) and protonated hydrotalcite ($[H-HT]^+$) species. Protonation of the epoxide with the $[H-HT]^+$ species, and subsequent reduction by the metal hydride species, followed by dehydration would provide the desired alkene product.

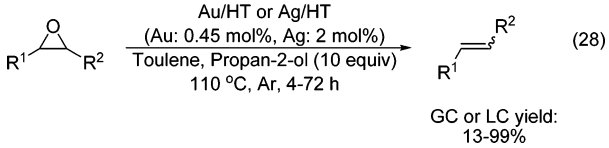

A core–shell nanocomposite of $Ag@CeO_2$ has been developed for the chemoselective reduction of nitrostyrenes and epoxides, while retaining C=C bonds (eqs 29 and 30).[31] This core–shell nanocomposite was shown to exhibit greater chemoselectivity than conventional oxide-supported Ag NPs. The enhanced chemoselectivity was due to the

maximization of the interfacial area between the Ag NPs and the basic CeO_2 shell in the core–shell structure (Figure 6). The exclusive formation of heterolytically cleaved H_2 species was achieved through a synergistic effect between Ag NPs and the basic sites of CeO_2, which suppressed the unfavorable formation of homolytically cleaved H_2 species on the bare Ag NPs. The resulting Ag hydride and proton species led to complete chemoselective reduction of polar functionalities while retaining the C=C bonds.

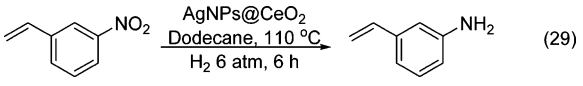

(29)

GC yield: 98%

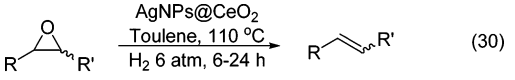

(30)

GC or LC yield:
94-98%

Ag NPs supported on hydroxyapatite (Ag/HAp) were utilized as active catalysts for the selective oxidation of silanes to silanols with water as the oxidant in the absence of organic solvents (eq 31).[32] The cooperative action between Ag NPs and HAp to create a hydrophilic environment played an important role in increasing the concentration of nucleophiles (OH^- or H_2O), hence promoting the formation of silanols by suppressing the condensation to disiloxanes. The catalyst could be recycled four times without any loss of activity.

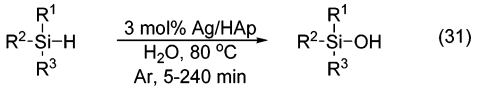

(31)

R^1, R^2, R^3 = Aryl or alkyl

GC conversion:
96-99%

We have established synthetic methodologies for the preparation of various transition metal NPs using a general phase-transfer protocol.[33] These methodologies allowed us to synthesize a variety of semiconductor–noble metal nanocomposites for electrochemical methanol oxidation reactions.[34] We have expanded this work to develop various semiconductor–gold nanocomposite systems (Figure 7), and shown that the PbS–Au nanocomposite was an efficient heterogeneous catalyst for the synthesis of propargylamines via a three-component coupling reaction of aldehyde, amine, and alkyne in water (eq 32).[35] The PbS–Au heterogeneous catalyst (supported on carbon) was stable to air and water, and could be easily recovered and reused. The particularly high catalytic activity of the

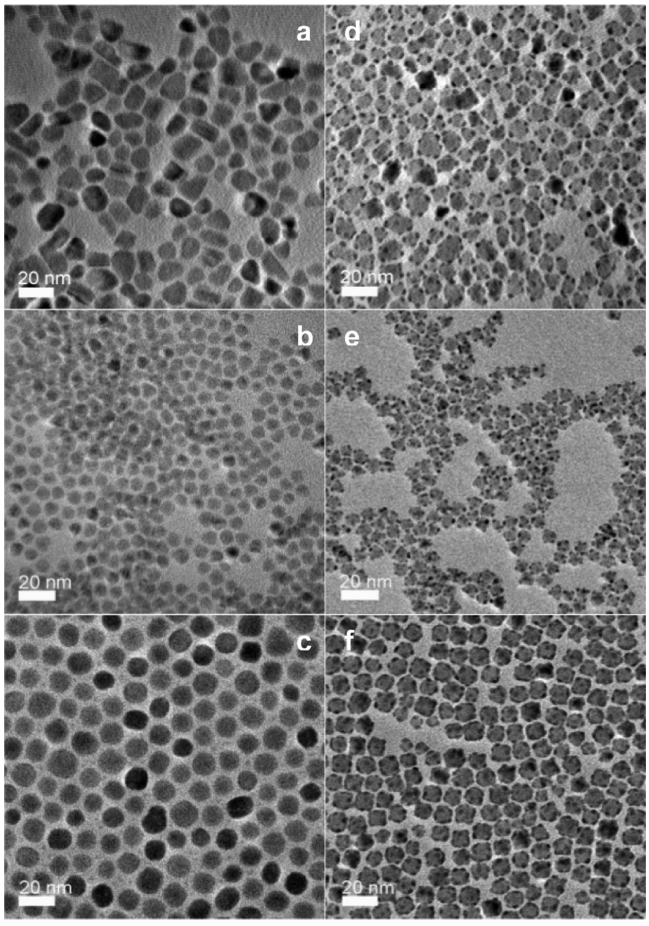

FIGURE 7. TEM image of (a) CdS, (b) CdSe, and (c) PbS quantum dots and (d) CdS–Au, (e) CdSe–Au, and (f) PbS–Au nanocomposites. Reprinted with permission from ref 35. Copyright 2009 Wiley-VCH Verlag GmbH & Co. KGaA.

PbS–Au nanocomposite for the three-component coupling reaction was attributed to the presence of Au(I) species on the semiconductor support.

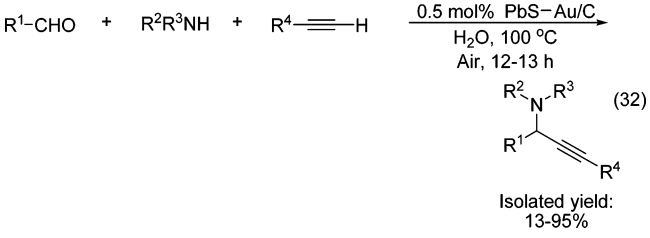

(32)

Isolated yield:
13-95%

Titania-supported Ir subnanoclusters (ca. 0.9 nm) have been employed as efficient heterogeneous catalysts for the direct tandem synthesis of quinolines from nitroarenes and aliphatic alcohols under mild and additive-free conditions (eq 33).[36] The high dispersion of subnanometer-sized Ir clusters and the acidic sites on titanium dioxide (TiO_2) surface were essential to the rapid domino synthesis of quinolines via a facile sequential transfer reduction–condensation–dehydrogenation pathway.

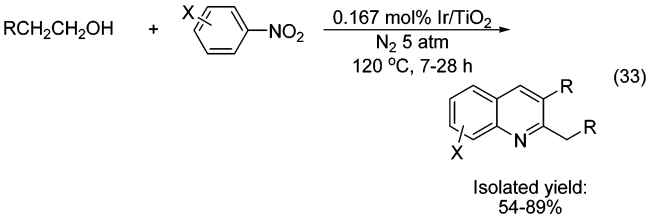

(33)

Hybrid Nanostructured Catalysts

An interesting strategy of applying heterogeneous catalyst to known homogeneous catalytic reactions was established by Witham et al.[37] Pt NPs were synthesized by either dendrimer or polymer encapsulation, followed by deposition on mesoporous silica SBA-15. The Pt NPs were then selectively oxidized by hypervalent iodine species, iodosobenzene dichloride ($PhICl_2$). The electrophilic Pt NPs thus produced could be used to catalyze a range of π-bond activation reactions previously accessible exclusively through homogeneous catalysis (eq 34). The catalyst was recycled four times with >90% yield of the product.

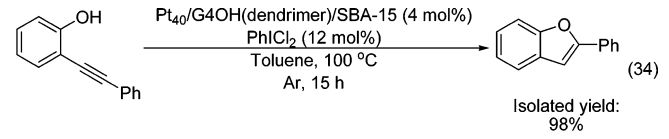

(34)

We have synthesized metallic and alloy NPs using polyoxometalates (POMs) as the reductants and stabilizing agents for electrochemical methanol oxidation.[38] This work was further extended to produce Pd−polyoxometalate nanomaterials supported on carbon (Pd−POM/C) for the efficient intermolecular C−C bond formation via C−H activation and C−N bond formation via oxidative amination, using O_2 as the terminal oxidant to produce substituted anilides and unsaturated amines, respectively (eqs 35 and 36).[39] The presence of POM was vital for the oxidative C−C and C−N coupling reactions since POM served as a reoxidation catalyst under O_2. The enhanced catalytic activity of the Pd−POM/C nanomaterials has been attributed to the presence of active Pd(II) species.

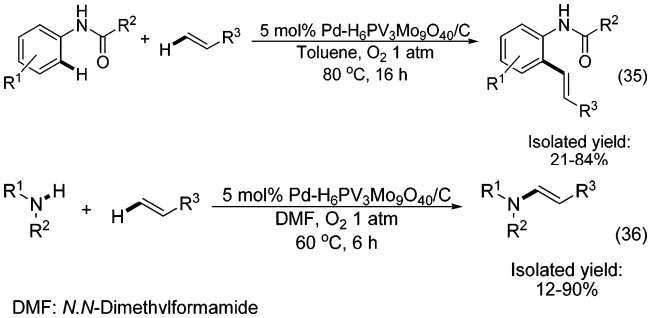

(35)

(36)

DMF: *N.N*-Dimethylformamide

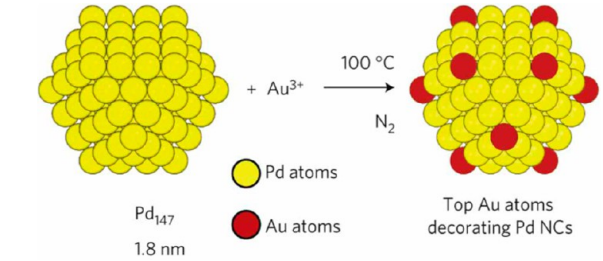

FIGURE 8. Schematic illustration of the deposition of top Au atoms on Pd mother clusters. Reprinted with permission from ref 42. Copyright 2012 Macmillan Publishers Ltd.: [Nature Materials].

Our laboratory has also developed a highly active and selective nanocomposite catalyst $Pt/WO_3/Al\text{-}ZrO_x$ for the C_{7+} paraffin isomerization at a low temperature of 125 °C.[40] This nanocomposite consisted of highly dispersed WO_3 domains and Pt clusters supported on Al-substituted ZrO_2 nanocrystals. The excellent catalytic performance of $Pt/WO_3/Al{-}ZrO_x$ was attributed to the high surface density of split-over H_2 and a more facile reverse process of H_2 spillover associated with the Al-doped ZrO_x, and the high dispersion of components in the nanocomposite catalyst.

An et al. recently reported the use of Keggin-type polyoxometalate-supported Au NPs ($Au/Cs_xH_{3-x}PW_{12}O_{40}$) for the selective conversion of cellobiose and cellulose to gluconic acid in water in the presence of O_2 (eq 37).[41] The acidity of the polyoxometalates and the mean size of the Au NPs played crucial roles in the selective conversion of cellobiose to gluconic acid. The acidic polyoxometalates not only catalyzed the hydrolysis of cellobiose to the glucose intermediate, but also contributed to the higher selectivity of gluconic acid by facilitating its desorption and inhibiting its further degradation.

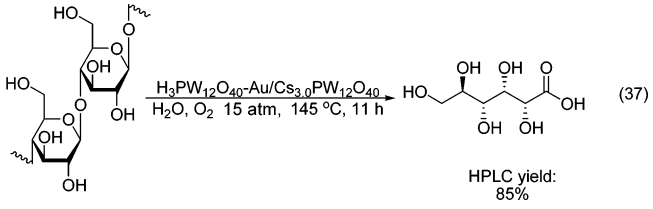

(37)

In a recent report by Zhang et al., active crown-jewel-structured Au/Pd nanocluster (CJ-Au/Pd NC) catalysts containing an abundance of top (vertex or corner) Au atoms (Figure 8) were synthesized by a galvanic replacement reaction.[42] The initial catalytic activity of the CJ-Au/Pd NCs for the aerobic glucose oxidation to gluconic acid (eq 38), normalized to the number of moles of Au, was much higher than Au. The high activity of the catalyst was attributed to

the donation of electrons from the Pd atoms to form negatively charged top Au atoms. Electron transfer from the anionic top Au atoms to O_2 would generate the active hydroperoxo-like species in the glucose oxidation.

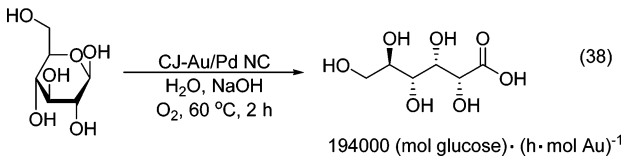

(38)

The use of isolated metal atom geometries was employed as a strategy for the selective hydrogenation of styrene and acetylene.[43] The authors found that individual isolated Pd atoms (1%) on a Cu surface activated H_2, which then spilled over onto the bare Cu(111) surface. The weakly bound hydrogen atoms in this system were effective in the selective hydrogenation of styrene and acetylene, as compared to the cases whereby pure Cu or Pd metal alone was employed.

Supported Au–Pd NPs on carbon or TiO_2 were used for the selective oxidation of primary benzylic carbon–hydrogen bonds in toluene with O_2 to benzyl benzoate under mild solvent-free conditions (eq 39).[44] The authors found that addition of Pd would lead to a substantial increase in the conversion, indicating a clear synergistic effect for the Au–Pd catalysts. The optimum catalyst composition has a Au/Pd molar ratio of 1:2. Au–Pd/C catalyst was found to be more active than Au–Pd/TiO_2 catalyst, which could be attributed to the particle/support wetting behavior and the availability of exposed corner/edge sites.

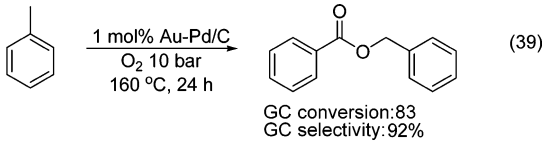

(39)

Polymer incarcerated carbon black (PICB) Au/Co NPs were synthesized as active catalyst for the selective synthesis of amides from alcohols and amines using O_2 as a terminal oxidant via a tandem oxidative process (eq 40).[45] The Au and Co NPs were well-dispersed throughout the polymer/carbon black composite material and were in close proximity to each other. The high activity and selectivity of the PICB Au/Co catalyst was due to the stabilization of the carbinolamine intermediate and the inhibition of undesirable dehydration side reaction by the Co center.

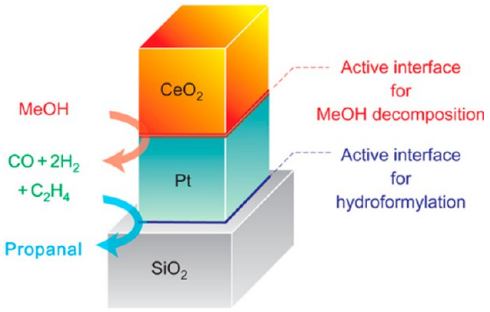

FIGURE 9. Ethylene hydroformylation with MeOH over a tandem catalyst. Reprinted with permission from ref 46. Copyright 2011 Macmillan Publishers Ltd.: [Nature Chemistry].

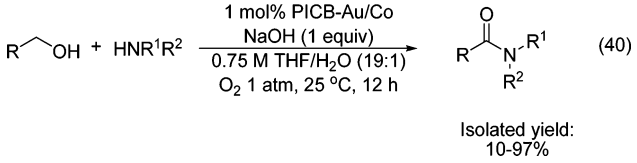

(40)

Nanocrystalline tandem catalysts with multiple metal–metal oxide interfaces were developed for catalytic sequential reactions.[46] A nanocrystal bilayer structure was fabricated by assembling Pt and CeO_2 nanocube monolayers on a flat SiO_2 substrate via the Langmuir–Blodgett method. The surface capping agents of the nanocrystals were removed by ultraviolet/ozone treatment to provide clean metal–metal oxide interfaces. Two separate sequential reactions were then catalyzed at the two distinct metal–metal oxide interfaces, CeO_2–Pt and Pt–SiO_2. The CeO_2–Pt interface decomposed methanol to form CO and H_2, which were then used for the catalysis of ethylene hydroformylation by the Pt–SiO_2 interface (Figure 9).

Conclusions and Outlook

Over the past few years, significant advances have been made in the synthesis of well-defined nanostructured materials as active heterogeneous catalysts for various types of organic transformations. These nanostructured materials have emerged as powerful catalysts for the efficient transformation of raw materials into valuable chemicals and fuels. Rational design of the size, shape, and composition of the active NPs, and the interface and architecture between the NPs and their support is critical to the development of highly active and selective nanocatalysts. This Account has reviewed selected examples of nanocatalysts to illustrate certain principles of catalytic enhancement via control of their dispersion, morphology, composition, oxidation state, and interaction with their supports. Although much progress has been made in the past decade, more research needs to

be conducted in the area of nanocatalysis. The challenge in the future of nanocatalyst research lies in the rational design and development of multifunctional, robust, and recyclable nanocomposite catalysts that can effectively perform multiple catalytic reactions with high atom-efficiencies, yields, chemoselectivities, and enantioselectivities within a one-pot system. The successful engineering of such versatile nanocomposites for low-temperature, low-pressure, and aqueous-based systems would present a significant step toward the attainment of green and sustainable chemical processes.

This work is supported by the Institute of Bioengineering and Nanotechnology (Biomedical Research Council, Agency for Science, Technology and Research, Singapore).

BIOGRAPHICAL INFORMATION

Leng Leng Chng received her Ph.D. from Stanford University. She is currently a Senior Research Scientist at the Institute of Bioengineering and Nanotechnology, Singapore, working on nanocatalysis and synthetic biomaterials.

Nandanan Erathodiyil received his Ph.D. from the National Chemical Laboratory affiliated with Pune University. He was a NIH Postdoctoral Fellow, Alexander von Humboldt Fellow, DOE-LBNL Post-Doctoral Scientist, and Senior Scientist at Molecular Therapeutics. As a Principal Research Scientist at the Institute of Bioengineering and Nanotechnology, Singapore, his research currently focuses on the development of synthetic biomaterials and nanocatalysis for sustainable organic reactions and energy applications.

Jackie Y. Ying received her Ph.D. from Princeton University. She was Professor of Chemical Engineering at Massachusetts Institute of Technology. She has been the Executive Director of the Institute of Bioengineering and Nanotechnology in Singapore since 2003. For her research on nanostructured materials, Prof. Ying has been recognized with the American Ceramic Society Ross C. Purdy Award, David and Lucile Packard Fellowship, Office of Naval Research and National Science Foundation Young Investigator Awards, Camille Dreyfus Teacher-Scholar Award, American Chemical Society Faculty Fellowship Award in Solid-State Chemistry, Technology Review TR100 Young Innovator Award, American Institute of Chemical Engineers (AIChE) Allan P. Colburn Award, Singapore National Institute of Chemistry-BASF Award in Materials Chemistry, Asian Innovation Silver Award, and International Union of Biochemistry and Molecular Biology (IUBMB) Jubilee Medal. Prof. Ying was elected a World Economic Forum Young Global Leader and a member of the German National Academy of Sciences, Leopoldina. She was named one of the "One Hundred Engineers of the Modern Era" by AIChE in its Centennial Celebration. She is the Editor-in-Chief of *Nano Today*.

FOOTNOTES

*To whom correspondence should be addressed. E-mail: jyying@ibn.a-star.edu.sg.
The authors declare no competing financial interest.

REFERENCES

1 (a) Ying, J. Y. Design and Synthesis of Nanostructured Catalysts. *Chem. Eng. Sci.* **2006**, *61*, 1540–1548. (b) Ying, J. Y. Nanostructural Tailoring: Opportunities for Molecular Engineering in Catalysis. *AIChE J.* **2000**, *46*, 1902–1906. (c) Narayanan, R.; El-Sayed, M. A. Catalysis with Transition Metal Nanoparticles in Colloidal Solution: Nanoparticle Shape Dependence and Stability. *J. Phys. Chem. B* **2005**, *109*, 12663–12676. (d) Schlögl, R.; Abd Hamid, S. B. Nanocatalysis: Mature Science Revisited or Something Really New? *Angew. Chem., Int. Ed.* **2004**, *43*, 1628–1637. (e) *Nanoparticles and Catalysis*; Astruc, D., Ed.; Wiley-VCH Verlag GmbH & Co. KGaA: Weinheim, 2008.

2 (a) Molnár, A. Efficient, Selective, and Recyclable Palladium Catalysts in Carbon-Carbon Coupling Reactions. *Chem. Rev.* **2011**, *111*, 2251–2320. (b) Polshettiwar, V.; Varma, R. S. Green Chemistry by Nano-Catalysis. *Green Chem.* **2010**, *12*, 743–754.

3 (a) Erathodiyil, N.; Ooi, S.; Seayad, A. M.; Han, Y.; Lee, S. S.; Ying, J. Y. Palladium Nanoclusters Supported on Propylurea-Modified Siliceous Mesocellular Foam for Coupling and Hydrogenation Reactions. *Chem.—Eur. J.* **2008**, *14*, 3118–3125. (b) Shakeri, M.; Tai, C.-W.; Göthelid, E.; Oscarsson, S.; Bäckwall, J.-E. Small Pd Nanoparticles Supported in Large Pores of Mesocellular Foam: An Excellent Catalyst for Racemization of Amines. *Chem.—Eur. J.* **2011**, *17*, 13269–13273. (c) Sawai, K.; Tatumi, R.; Nakahodo, T.; Fujihara, H. Asymmetric Suzuki-Miyaura Coupling Reactions Catalyzed by Chiral Palladium Nanoparticles at Room Temperature. *Angew. Chem., Int. Ed.* **2008**, *47*, 6917–6919. (d) Dhakshinamoorthy, A.; Garcia, H. Catalysis by Metal Nanoparticles Embedded on Metal−Organic Frameworks. *Chem. Soc. Rev.* **2012**, *41*, 5262–5284.

4 Crespo-Quesada, M.; Yarulin, A.; Jin, M.; Xia, Y.; Kiwi-Minker, L. Structure Sensitivity of Alkynol Hydrogenation on Shape- and Size-Controlled Palladium Nanocrystals: Which Sites are Most Active and Selective? *J. Am. Chem. Soc.* **2011**, *133*, 12787–12794.

5 Mostafa, S.; Behafarid, F.; Croy, J. R.; Ono, L. K.; Li, L.; Yang, J. C.; Frenkel, A. I.; Cuenya, B. R. Shape-Dependent Catalytic Properties of Pt Nanoparticles. *J. Am. Chem. Soc.* **2010**, *132*, 15714–15719.

6 Hong, H.; Hu, L.; Li, M.; Zheng, J.; Sun, X.; Lu, X.; Cao, X.; Lu, J.; Gu, H. Preparation of $Pt@Fe_2O_3$ Nanowires and their Catalysis of Selective Oxidation of Olefins and Alcohols. *Chem.—Eur. J.* **2011**, *17*, 8726–8730.

7 (a) Blaser, H.-U.; Studer, M. Cinchona-Modified Platinum Catalysts: From Ligand Acceleration to Technical Processes. *Acc. Chem. Res.* **2007**, *40*, 1348–1356. (b) Gual, A.; Godard, C.; Castillón, S.; Claver, C. Soluble Transition-Metal Nanoparticles-Catalyzed Hydrogenation of Arenes. *Dalton Trans.* **2010**, *39*, 11499–11512.

8 Schmidt, E.; Vargas, A.; Mallat, T.; Baiker, A. Shape-Selective Enantioselective Hydrogenation on Pt Nanoparticles. *J. Am. Chem. Soc.* **2009**, *131*, 12358–12367.

9 Wu, Y.; Cai, S.; Wang, D.; He, W.; Li, Y. Synthesis of Water-Soluble Octahedral, Truncated Octahedral and Cubic Pt-Ni Nanocrystals and Their Structure-Activity Study in Model Hydrogenation Reactions. *J. Am. Chem. Soc.* **2012**, *134*, 8975–8981.

10 Erathodiyil, N.; Gu, H.; Shao, H.; Jiang, J.; Ying, J. Y. Enantioselective Hydrogenation of α-Ketoesters Over Alkaloid-Modified Platinum Nanowires. *Green Chem.* **2011**, *13*, 3070–3074.

11 Hu, L.; Cao, X.; Ge, D.; Hong, H.; Guo, Z.; Chen, L.; Sun, X.; Tang, J.; Zheng, J.; Lu, J.; Gu, H. Ultrathin Platinum Nanowire Catalysts for Direct C-N Coupling of Carbonyls with Aromatic Nitro Compounds under 1 bar Hydrogen. *Chem.—Eur. J.* **2011**, *17*, 14283–14287.

12 Xu, Y.; Wang, H.; Yu, Y.; Tian, L.; Zhao, W.; Zhang, B. Cu_2O Nanocrystals: Surfactant-Free Room-Temperature Morphology-Modulated Synthesis and Shape-Dependent Heterogeneous Organic Catalytic Activities. *J. Phys. Chem. C* **2011**, *115*, 15288–15296.

13 Jin, M.; Zhang, H.; Xie, Z.; Xia, Y. Palladium Concave Nanocubes with High-Index Facets and Their Enhanced Catalytic Properties. *Angew. Chem., Int. Ed.* **2011**, *50*, 7850–7854.

14 Polshettiwar, V.; Luque, R.; Fihri, A.; Zhu, H.; Bouhrara, M.; Basset, J.-M. Magnetically Recoverable Nanocatalysts. *Chem. Rev.* **2011**, *111*, 3036–3075.

15 (a) Zhu, Y.; Stubbs, L. P.; Ho, F.; Liu, R.; Ship, C. P.; Maguire, J. A.; Hosmane, N. S. Magnetic Nanocomposites: A New Perspective in Catalysis. *ChemCatChem* **2010**, *2*, 365–374. (b) Shylesh, S.; Schünemann, V.; Thiel, W. R. Magnetically Separable Nanocatalysts: Bridges Between Homogeneous and Heterogeneous Catalysts. *Angew. Chem., Int. Ed.* **2010**, *49*, 3428–3459.

16 Yi, D. K.; Lee, S. S.; Ying, J. Y. Synthesis and Applications of Magnetic Nanocomposite Catalysts. *Chem. Mater.* **2006**, *18*, 2459–2461.

17 Lee, S. S.; Riduan, S. N.; Erathodiyil, N.; Lim, J.; Cheong, J. L.; Cha, J.; Han, Y.; Ying, J. Y. Magnetic Nanoparticles Entrapped in Siliceous Mesocellular Foam: A New Catalyst Support. *Chem.—Eur. J.* **2012**, *18*, 7394–7403.

18 (a) Zhou, L.; Gao, C.; Xu, W. Robust Fe_3O_4/SiO_2-Pt/Au/Pd Magnetic Nanocatalysts with Multifunctional Hyperbranched Polyglycerol Amplifiers. *Langmuir* **2010**, *26*, 11217–11225. (b) Lin, F.-H.; Doong, R.-A. Bifunctional Au-Fe_3O_4 Heterostructures for Magnetically Recyclable Catalysis of Nitrophenol Reduction. *J. Phys. Chem. C* **2011**, *115*, 6591–6598. (c) Ko, S.; Jang, J. A Highly Efficient Palladium Nanocatalyst Anchored on a Magnetically Functionalized Polymer-Nanotube Support. *Angew. Chem., Int. Ed.* **2006**, *45*, 7564–7567.

19 Anand, N.; Reddy, K. H. P.; Satyanarayana, T.; Rao, K. S. R.; Burri, D. R. A Magnetically Recoverable γ-Fe_2O_3 Nanocatalyst for the Synthesis of 2-Phenylquinazolines Under Solvent-Free Conditions. *Catal. Sci. Technol.* **2012**, *2*, 570–574.

20 Park, J. C.; Lee, H. J.; Jung, H. S.; Kim, M.; Kim., H. J.; Park, K. H.; Song, H. Gram-Scale Synthesis of Magnetically Separable and Recyclable Co@SiO_2 Yolk-Shell Nanocatalysts for Phenoxycarbonylation Reactions. *ChemCatChem* **2011**, *3*, 755–760.

21 Polshettiwar, V.; Varma, R. S. Nanoparticle-Supported and Magnetically Recoverable Ruthenium Hydroxide Catalyst: Efficient Hydration of Nitriles to Amides in Aqueous Medium. *Chem.—Eur. J.* **2009**, *15*, 1582–1586.

22 Hudson, R.; Li, C.-J.; Moores, A. Magnetic Copper-Iron Nanoparticles as Simple Heterogeneous Catalysts for the Azide-Alkyne Click Reaction in Water. *Green Chem.* **2012**, *14*, 622–624.

23 Swapna, K.; Murthy, S, N.; Nageswar, Y. V. D. Magnetically Separable and Resuable Copper Ferrite Nanoparticles for Cross-Coupling of Aryl Halides and Diphenyl Diselenide. *Eur. J. Org. Chem.* **2011**, 1940–1946.

24 Ranganath, K. V. S.; Kloesges, J.; Schäfer, A. H.; Glorius, F. Asymmetric Nanocatalysis: N-Heterocyclic Carbenes as Chiral Modifiers of Fe_3O_4/Pd Nanoparticles. *Angew. Chem., Int. Ed.* **2010**, *49*, 7786–7789.

25 Hu, A.; Liu, S.; Lin, W. Immobilization of Chiral Catalysts on Magnetic Nanoparticles for Highly Enantioselective Asymmetric Hydrogenation of Aromatic Ketones. *RSC Adv.* **2012**, *2*, 2576–2580.

26 Mori, K.; Kondo, Y.; Yamashita, H. Synthesis and Characterization of FePd Magnetic Nanoparticles Modified with Chiral BINAP Ligand as a Recoverable Catalyst Vehicle for the Asymmetric Coupling Reaction. *Phys. Chem. Chem. Phys.* **2009**, *11*, 8949–8954.

27 Zhang, X.; Corma, A. Supported Gold(III) Catalysts for Highly Efficient Three-Component Coupling Reactions. *Angew. Chem., Int. Ed.* **2008**, *47*, 4358–4361.

28 Wang, F.; Ueda, W.; Xu, J. Detection and Measurement of Surface Electron Transfer on Reduced Molybdenum Oxides (MoO_x) and Catalytic Activities of Au/MoO_x. *Angew. Chem., Int. Ed.* **2012**, *51*, 3883–3887.

29 Tsunoyama, H.; Ichikuni, N.; Sakurai, H.; Tsukuda, T. Effect of Electronic Structures of Au Clusters Stabilized by Poly(N-vinyl-2-pyrrolidone) on Aerobic Oxidation Catalysis. *J. Am. Chem. Soc.* **2009**, *131*, 7086–7093.

30 Mitsudome, T.; Noujima, A.; Mikami, Y.; Mizugaki, T.; Jitsukawa, K.; Kaneda, K. Supported Gold and Silver Nanoparticles for Catalytic Deoxygenation of Epoxides into Alkenes. *Angew. Chem., Int. Ed.* **2010**, *49*, 5545–5548.

31 Mitsudome, T.; Mikami, Y.; Matoba, M.; Mizugaki, T.; Jitsukawa, K.; Kaneda, K. Design of a Silver-Cerium Dioxide Core-Shell Nanocomposite Catalyst for Chemoselective Reduction Reactions. *Angew. Chem., Int. Ed.* **2012**, *51*, 136–139.

32 Mitsudome, T.; Arita, S.; Mori, H.; Mizugaki, T.; Jitsukawa, K.; Kaneda, K. Supported Silver-Nanoparticle-Catalyzed Highly Efficient Aqueous Oxidation of Phenylsilanes to Silanols. *Angew. Chem., Int. Ed.* **2008**, *47*, 7938–7940.

33 (a) Yang, J.; Sargent, E.; Kelley, S.; Ying, J. Y. A General Phase-Transfer Protocol for Metal Ions and Its Application in Nanocrystal Synthesis. *Nat. Mater.* **2009**, *8*, 683–689. (b) Yang, J.; Lee, J. Y.; Ying, J. Y. Phase Transfer and Its Applications in Nanotechnology. *Chem. Soc. Rev.* **2011**, *40*, 1672–1696.

34 Yang, J.; Ying, J. Y. Nanocomposites of Ag_2S and Noble Metals. *Angew. Chem., Int. Ed.* **2011**, *50*, 4637–4643.

35 Chng, L. L.; Yang, J.; Wei, Y.; Ying, J. Y. Semiconductor-Gold Nanocomposite Catalysts for the Efficient Three-Component Coupling of Aldehyde, Amine and Alkyne in Water. *Adv. Synth. Catal.* **2009**, *351*, 2887–2896.

36 He, L.; Wang, J.-Q.; Gong, Y.; Liu, Y.-M.; Cao, Y.; He, H.-Y.; Fan, K.-N. Titania-Supported Iridium Subnanoclusters as an Efficient Heterogeneous Catalyst for Direct Synthesis of Quinolines from Nitroarenes and Aliphatic Alcohols. *Angew. Chem., Int. Ed.* **2011**, *50*, 10216–10220.

37 Witham, C. A.; Huang, W.; Tsung, C.-K.; Kuhn, J. N.; Somorjai, G. A.; Toste, F. D. Converting Homogeneous to Heterogeneous in Electrophilic Catalysis Using Monodisperse Metal Nanoparticles. *Nat. Chem.* **2010**, *2*, 36–41.

38 Zhang, J.; Ting, B. P.; Koh, Y. T.; Ying, J. Y. Synthesis of Metallic Nanoparticles Using Electrogenerated Reduced Forms of $[\alpha\text{-}SiW_{12}O_{40}]^{4-}$ as Both Reductants and Stabilizing Agents. *Chem. Mater.* **2011**, *23*, 4688–4693.

39 Chng, L. L.; Zhang, J.; Yang, J.; Amoura, M.; Ying, J. Y. C-C Bond Formation via C-H Activation and C-N Bond Formation via Oxidative Amination Catalyzed by Palladium-Polyoxometalate Nanomaterials Using Dioxygen as the Terminal Oxidant. *Adv. Synth. Catal.* **2011**, *353*, 2988–2998.

40 Xu, J.; Ying, J. Y. A Highly Active and Selective Nanocomposite Catalyst for C_{7+} Paraffin Isomerization. *Angew. Chem., Int. Ed.* **2006**, *45*, 6700–6704.

41 An, D.; Ye, A.; Deng, W.; Zhang, Q.; Wang, Y. Selective Conversion of Cellobiose and Cellulose into Gluconic Acid in Water in the Presence of Oxygen, Catalyzed by Polyoxometalate-Supported Gold Nanoparticles. *Chem.—Eur. J.* **2012**, *18*, 2938–2947.

42 Zhang, H.; Watanabe, T.; Okumura, M.; Haruta, M.; Toshima, N. Catalytically Highly Active Top Gold Atom on Palladium Nanocluster. *Nat. Mater.* **2012**, *11*, 49–52.

43 Kyriakou, G.; Boucher, M. B.; Jewell, A. D.; Lewis, E. A.; Lawton, T. J.; Baber, A. E.; Tierney, H. L.; Flytzani-Stephanopoulos, M.; Sykes, E. C. H. Isolated Metal Atom Geometries as a Strategy for Selective Heterogeneous Hydrogenations. *Science* **2012**, *335*, 1209–1212.

44 Kesavan, L.; Tiruvalam, R.; Ab Rahim, M. H.; Saiman, M. I. B.; Enache, D. I.; Jenkins, R. L.; Dimitratos, N.; Lopez-Sanchez, J. A.; Taylor, S. H.; Knight, D. W.; Kiely, C. J.; Hutchings, G. J. Solvent-Free Oxidation of Primary Carbon-Hydrogen Bonds in Toluene Using Au-Pd Alloy Nanoparticles. *Science* **2011**, *331*, 195–199.

45 Soulé, J.-F.; Miyamura, H.; Kobayashi, S. Powerful Amide Synthesis from Alcohols and Amines under Aerobic Conditions Catalyzed by Gold or Gold/Iron, -Nickel or -Cobalt Nanoparticles. *J. Am. Chem. Soc.* **2011**, *133*, 18550–18553.

46 Yamada, Y.; Tsung, C.-K.; Huang, W.; Huo, Z.; Habas, S. E.; Soejima, T.; Aliaga, C. E.; Somorjai, G. A.; Yang, P. Nanocrystal Bilayer for Tandem Catalysis. *Nat. Chem.* **2011**, *3*, 372–376.